

Published in final edited form as:

Adv Mater. 2013 August 14; 25(30): 4107–4112. doi:10.1002/adma.201301658.

Fabrication of 3-D Microstructures from the Interactions of Immiscible Liquids with a Structured Surface

Joseph J. Balowski¹, Yuli Wang¹, and Nancy L. Allbritton^{1,2,*}

¹Department of Chemistry University of North Carolina Chapel Hill, NC 27599, USA

²Department of Biomedical Engineering University of North Carolina, Chapel Hill, NC 27599 and North Carolina State University, Raleigh, NC 27695, USA

Three-dimensional (3-D) micron-sized structures have found widespread application in microelectronics, photonics, and biotechnology.^[1–3] Conventional microfabrication techniques, particularly photolithography and soft lithography, are well-suited to the production of two-dimensional (2-D) microstructures with precisely controlled patterns along an x- and y-axis.^[4,5] Rudimentary three-dimensional (3-D) structures can be formed by projecting these 2-D patterns some fixed distance along a z-axis. Truly complex 3-D microstructures, however, require specialized extensions of these methods or other independent techniques.^[6] Photolithographic strategies such as gray-scale photolithography, multiphoton lithography, and interference lithography fabricate high resolution 3-D structures, but generally require light-activated materials and sophisticated infrastructure.^[7–9] Direct layer-by-layer placement or removal of materials, for example, stereolithography, 3-D printing, and laser ablation, typically exhibit low feature resolution, low throughput, or require specialized and expensive instrumentation.^[10–12] Here we present a strategy termed liquid lithography which, using no pattern-alignment steps or dedicated equipment, can nevertheless rapidly and efficiently construct intricate 3-D assemblies.

Interfacial tension present at the boundary between two immiscible liquids acts to minimize their contact area. In an isolated system of two immiscible liquids, the shape assumed by the liquid of lesser volume is that of a sphere (or droplet). If a solid, flat surface is introduced and the droplet is made to “wet” that surface partially, the shape produced is a truncated sphere (Figure 1a), or a truncated spherical “microwell” in the matrix liquid.^[13] Surface energy modification can be performed to manipulate the wetting properties of liquids on the flat substrate, in a sense *stretching* the truncated spheres into elongated shapes such as hemicylindrical microchannels.^[14] However, the complexity of surfaces generated by these methods is ultimately very limited. Significantly greater complexity can arise when substrate geometry, rather than surface chemistry, is used as the primary mechanism to direct placement of the liquid-liquid interface.

In liquid lithography, a geometrically-patterned substrate serves two purposes. First, it acts as a boundary for the immiscible liquids interacting with its surface. More fundamentally, it serves to direct placement of their liquid-liquid interface. Solidification and retrieval of one of the immiscible liquids reveals the topographical features encoded by the multicomponent system.

*nlallbri@unc.edu.

Supporting Information is available online from Wiley InterScience.

We begin with a simple example, the conversion of an array of cylindrical microwells to an array of micropillars terminated in smooth, spherically-curved concave and convex surfaces (Figure 1c–h). An isolated droplet of a “first liquid” is deposited in each microwell of the array through the simple, rapid, highly-parallel process of discontinuous dewetting.^[15] The entire array is covered with a solution of the first liquid in a volatile solvent, and the excess (all that is not physically trapped in the microwells) is drained away. The solvent is evaporated with a short low-temperature bake. A “second liquid,” immiscible with the first, is then added to cover the entire array, replacing the liquid-air interfaces with liquid-liquid interfaces. The liquid-liquid interfaces define “micro-menisci.” Solidification and retrieval of the second liquid produces an array of meniscus-terminated micropillars (Figure 1h), which can be used as microlens arrays^[16] (Figure S1), while the curved bottoms of replica-molded microwell arrays (Figure 1i, Figure 2a–j) can be used for cell culture.^[17]

To generate the meniscus terminated microwell/micropillar structures shown here, polyhydric alcohols (“polyols”) were used as first liquids, with dewetting solutions consisting of roughly equal mixtures of polyols and water. Polydimethylsiloxane (PDMS) prepolymer was used as the second liquid. Cylindrical microwell array substrates were fabricated from the negative photoresist SU-8 by standard photolithography and used as is, or after *in vacuo* surface treatment with octyl- or ethyltrichlorosilane. SU8 photolithography is common practice in the microfabrication community, and soft lithography of PDMS is nearly ubiquitous. While not regularly employed in conventional lithographies, polyols are commonly used in other laboratory operations, and in general this class of chemicals is nontoxic, inexpensive, and highly water-soluble.

The direction and magnitude of curvature for these micro-menisci are determined by the contact angle of the polyol/PDMS/substrate system (Figure 1a,b). The contact angle is in turn controlled by the interfacial tensions at the liquid-liquid and liquid-solid interfaces according to Young's equation:

$$\cos(\theta) = \frac{\gamma_{PDMS/substrate} - \gamma_{polyol/substrate}}{\gamma_{PDMS/polyol}} \quad (1)$$

Interfacial tensions for the liquid-liquid and liquid-solid combinations used here are not available in the literature and are difficult to determine empirically. Fortunately, the surface energies (i.e. the interfacial tension *against air*) of most of the liquids and solid surfaces one would wish to employ in this lithography method are available, and these parameters can be used along with Young's equation to make accurate qualitative predictions about wetting behavior. When the difference in surface energy of two phases is small, the interfacial tension between the two is generally also small, especially when the two phases are chemically similar.^[18] Conversely, when the surface energy of one phase is much greater than the surface energy of its partner, the interfacial tension tends to be large.

From equation (1) it can be observed that as the interfacial tension between the polyol and the substrate ($\gamma_{polyol/substrate}$) goes to zero, $\cos(\theta)$ tends toward positive values, yielding $<90^\circ$ contact angles. Thus, when the polyol and the substrate have similar surface energies, $\gamma_{polyol/substrate}$ is low, and “wetting” behavior is observed. Similarly, small surface energy differences between PDMS and the substrate are correlated with small $\gamma_{PDMS/substrate}$ values, negative $\cos(\theta)$ values ($>90^\circ$), and “non-wetting” behavior of the polyol.

Contact angle control via surface energy manipulation was demonstrated using the transformation of cylindrical microwells to meniscus-terminated micropillars/microwells (Figure 2). The non-wetting condition was observed with octyltrichlorosilane-treated SU-8

substrates (surface energy 22.9 mN m^{-1}), since both it and the “second liquid” PDMS (20.8 mN m^{-1}) had roughly the same surface energy, and presumably a low interfacial tension ($\gamma_{\text{PDMS/substrate}}$). Wetting was generally observed for the higher surface energy untreated SU-8 substrates (45.2 mN m^{-1}),^[19] while both wetting and non-wetting behavior was observed for intermediate surface energy ethyltrichlorosilane-treated SU-8 (34.1 mN m^{-1}).

Although in theory, it is possible to modify the surface energy of any of the three phases, in practice, for the combination of liquids and substrates used above, it is most convenient to modify the properties of the SU-8 substrate and the polyol first liquid. “Digital” control of contact angle could be effected by use of specific combinations of substrate surface treatment and a pure polyol (Figure 2k). “Analog” modulation was obtained through use of mixtures of two miscible polyols (Figure 2l). By varying the ratio at which the two materials are mixed, a binary polyol with any surface energy between that of the two pure materials can be produced—increasing the polyol surface energy indirectly modifies the polyol-associated interfacial tensions ($\gamma_{\text{polyol/substrate}}$ and $\gamma_{\text{PDMS/polyol}}$), generally increasing both terms while $\gamma_{\text{PDMS/substrate}}$ is held constant, resulting in θ being pushed incrementally towards larger values. The overlap in contact angle range for each substrate type (Figure 2k), coupled with the precise control of contact angle afforded by the use of binary polyol mixtures (Figure 2l), means that the entire range of contact angles (and meniscus curvatures) from the extremes of Figure 2a (5°) to 2e (160°) are accessible using this set of three common materials. The $0\text{--}5^\circ$ and $160\text{--}180^\circ$ range can be spanned by use of different liquids and/or substrates or surface treatments.

Altering the polyol fill volume and substrate geometry yielded additional topographic features (Figure 3) using the same fabrication procedure outlined in Figure 1c–i. These are but a few examples of the wide range of structures that can be produced and may find use as fasteners, adhesives, microcontainers, photonics and fluidic components.^[20–22] Fabrication details are given in the Supporting Information.

As is typical of liquid lithography, the resulting final product features are similar to, but distinct from, the features present on the substrate. Although still geometrically modest, microstructures like those presented in Figure 3 are challenging if not impossible to produce in standard microfabrication laboratories which lack advanced lithographic equipment (e.g. micro-stereolithography).^[23] Even *with* such equipment, these structures can only be made out of a very limited set of materials, usually at high cost and with low throughput. Liquid lithography allows production of structures with smooth curved surfaces and cavities of well-defined size and placement, starting from substrate structures without these features (such as the straight side-walled, “prismatic” structures produced by standard photolithography or CNC milling). Thus, in these examples, liquid lithography can be thought of as a simple method of extending the range of structures which can be produced in an individual microfabrication laboratory given the restraints of what specific lithography techniques and capabilities are available. Additionally, simple microwell and microchannel molds, such as those used in the production of the Figure 3 structures, can also be obtained from commercial foundries so that liquid lithography, like soft lithography, should be readily accessible to most labs.

In all cases presented thus far, an SU-8 substrate, a polyol first liquid, and PDMS prepolymer second liquid were used to effect liquid lithography with the transformation recorded in the solidified PDMS. These materials were chosen due to their familiarity within the micro-fabrication community and their easy incorporation into this molding method, but the method is not reliant on them. Further, either of the immiscible liquids is a candidate for solidification. Varying the materials, solidified layer and/or substrate geometry can lead to

increasingly intricate microstructures. A notable example is the use of a solidifiable liquid in place of the polyol and the application of a very high surface energy, sacrificial liquid in place of the PDMS prepolymer. Sorbitol (glucose sugar alcohol) was used as the high surface energy “second” liquid since it is inexpensive, non-toxic, and highly water-soluble. Initially, SU-8 was employed as the solidifiable “first” liquid. Fully-cured PDMS elastomer formed the substrate. Solutions of SU-8 in gamma-butyrolactone (GBL) were deposited on the substrate, followed by dewetting and baking to remove solvent. Sorbitol was overlaid and thermal reflow of SU-8 was initiated (Figure 4a–c). Solidification of the SU-8 was achieved by a phase change from liquid to solid upon cooling to room temperature, and exposure to UV light chemically cross-linked the material for added strength.

The high surface energy of the sorbitol yielded large second-liquid-associated interfacial tensions [$\gamma_{\text{sorbitol/substrate}}$ and $\gamma_{\text{sorbitol/SU-8}}$, equation (2)], driving $\cos \theta$ towards 1.0 and a contact angle of 0° (i.e. “perfect wetting”). Areas of the substrate which contained high surface-area-to-volume (SA/V) ratio features were wetted preferentially, and SU-8 was effectively “pushed” into the edges and grooves of the substrate structure (Figure 4a,c). Even with a simple substrate geometry (a triangular microwell array), relatively complex multi-level structures could be produced (Figure 4d,e).

$$\cos(\theta) = \frac{\gamma_{\text{sorbitol/substrate}} - \gamma_{\text{SU8/substrate}}}{\gamma_{\text{sorbitol/SU8}}} \quad (2)$$

Structures which bear progressively diminished resemblance to the initial substrate mold can be formed by utilizing sequential rounds of liquid lithography wherein the product of the first stage forms the structured substrate for the second stage. As a demonstration, we created an array of micrometer-scale rotundas (Figure 4h,i, Figure S3). Many other sophisticated structures can similarly be built by performing sequential liquid lithography or by employing more than two immiscible liquids.

To demonstrate the diversity of materials suitable for liquid lithography, a complex microfabricated “mesh” structure was produced from the biodegradable thermoplastic poly(DL-lactide) (PDLLA) using the same “groove-filling” phenomenon discussed above. The mesh consisted of an array of micro-baskets set within a plane (Figure 4f,g). The entire face of the mesh was covered in pores of $15 \mu\text{m}$ or less, and the thickness of the PDLLA did not exceed $20 \mu\text{m}$ at any point. Both pore size and thickness can be further reduced, and more elaborate architectures are possible using the same simple, rapid, low-waste process (see Supporting Information). Template patterns were defined by three-layer photolithography. PDMS substrates were produced from these photoresist templates by soft lithography (at minimum dozens of such substrates can be made in this manner). One PDMS substrate was used to make forty of these mesh structures, with no damage to the substrate features. Taken together, these two ‘pattern amplification’ steps allow a large number of final products to be manufactured via liquid lithography, diluting the cost of producing the complex, multi-level substrate template as production volume increases. These structures may find use in the formation of intricately patterned, biodegradable scaffolding, for example, in tissue engineering.^[24] Similar structures were also fabricated from polystyrene (Figure S2).

Although polymerizable monomer/prepolymer materials can be manipulated in the same manner, the ability to pattern high MW thermoplastic polymers directly permits use of materials familiar to biological study (e.g. polystyrene).^[25] Additionally, while this method is similar to soft lithography in the cost and ease of making micro-structured cell culture surfaces, our technique can readily make use of materials besides PDMS, which is

increasingly being recognized for its propensity to leach unreacted oligomers into the cell culture medium, and to absorb small, hydrophobic molecules into its porous matrix.^[24–27] Many micro-fabricated “organ-on-a-chip” devices incorporate flat, micro-porous membrane components, which allow diffusion of molecular species across the membrane and co-culture of different cell types on opposing faces.^[28–31] However, cells in many tissues are present in a configuration of 3D micrometer-scale topography. This method allows production of porous membranes which retain their ability to co-culture complementary cell types, while presenting *in-vivo*-like local topography, even as global (macro-scale) planarity is maintained, allowing imaging of the entire array by conventional microscopy methods. Although it's known that some cell types recognize and respond to 3D micro-scale structure,^[32–34] further study is required to determine if *in vivo*-like local micro-topography could enhance the physiological mimicry of cells grown on these porous membrane scaffolds.

We have developed an alignment-free method capable of rapidly and inexpensively producing arrays of intricate microstructures. Liquid lithography is flexible from a materials standpoint, working well with thermoset polymers, solvent-processible thermoplastics, and other photoactive and non-photoactive materials. The structured substrates may be fabricated out of a variety of substances by conventional photolithography, soft lithography, CNC drilling, 3-D printing or other methods.

The particular structures shown in this work are not a comprehensive set. Liquid types and volumes, as well as substrate surface energies and geometries can be programmed to permit a greatly expanded portfolio of microstructures. Computational modeling should enable formation of increasingly sophisticated structures, although for basic substrate geometries predictions of the liquid interface topography can be made intuitively without elaborate calculations. We expect liquid lithography to find immediate use as a simple means of expanding the range of structures that can be fabricated in laboratories equipped with standard lithography instrumentation. In the longer term, we believe that the speed and economy by which this method produces microstructures, along with its significant materials possibilities, will allow this technology to find substantial applications in a multiplicity of fields.

Experimental Section

SU-8 photoresist substrates were produced through standard photolithography. Surfaces were modified by exposure to either ethyl- or octyltrichlorosilane *in vacuo* for >3 hours. PDMS substrates were produced via soft lithography^[5] using photoresist templates.

Substrates with recessed microstructures were charged with first liquid through discontinuous dewetting [15]. Dewetting occurred on flat surfaces outside of raised microstructure arrays, while the arrays themselves pinned macroscopic “droplets,” 1 mm tall, existing continuously between (and sometimes above) the raised features.

First liquid solutions were composed of: 10, 20, 25 or 40% w/w mixtures of one or two polyol materials in water; 5, 25 or 50% SU-8 in GBL; or 25% PDLLA or poly(styrene) in gamma-valerolactone (GVL). After substrates were charged with first liquid (solution), the volatile solvent, when present, was baked away before (polyols and SU8) or after (PDLLA and PS) overlay of second liquid.

Meniscus-terminated micropillars were produced using treated and untreated SU8 microwell array substrates, PDMS prepolymer second liquid, and polyol first liquid (dipropylene glycol, tetraethylene glycol, 1,2,6-hexanetriol, glycerol, D-ribose, or sorbitol, 40% w/w in water). After discontinuous dewetting, water was removed by a 65 °C bake for 4–20 min.

PDMS was overlaid and exposed to vacuum for 30 s to remove air trapped between the polyol surface and microwell opening. PDMS was cured at 65 °C for 1–2 hr, demolded, rinsed with DI water and baked at 120 °C for 30 min. Meniscus-terminated microwells (Figure 2a–j) were produced from the micropillars through soft lithography. The structures in Figure 3c–j were produced similarly, without the replica molding step, using 10, 20, 25, 40 or 100% tetraethylene glycol or glycerol solutions (see Supporting Information).

SU-8, PDLA and PS structures were produced using molten sorbitol second liquid (120 °C) and fully-cured PDMS substrates. In SU-8 molding, substrates were charged with SU-8 solutions, and baked at 95 °C 60 min to remove solvent; SU-8 was reshaped around bulk overlaid sorbitol (Figure 4c) or sorbitol micro-droplets (Figure d,e,h,i) by heating to 120 °C for 30 min. After cooling to room temperature, the SU-8 was cross-linked by exposing to 400 mJ cm⁻² UV light. SU-8 microparticles were extracted from the substrate in array form by attaching their “tops” to an epoxy slab before demolding (Figure d,e,h,i) and washing out the sorbitol droplets. In PDLA and PS molding, molten sorbitol was overlaid within 1 minute of the dewetting step, and heated for 15 min at 120 °C to remove solvent. The thin, delicate polymer “mesh” structures (Figure 4f,g, Figure S3) were cleaned of overlaying sorbitol with DI water, and covered with a conformal film of water soluble polymer to serve as a rigid backing during demolding. The backings were later dissolved in DI water. Details are provided in the Supporting Information.

Supplementary Material

Refer to Web version on PubMed Central for supplementary material.

Acknowledgments

This work was supported by a grant from the National Institutes of Health (EB012549). We would like to thank Colleen Phillips for technical support, and Michelle Kovarik and Nicholas Dobes for helpful discussions. We also acknowledge Wallace Ambrose and Robert Geil in the Chapel Hill Analytical and Nanofabrication Laboratory for assistance with electron microscopy and fabrication methods. We thank Pavak Shah for photography of the UNC rotunda.

References

- [1]. Lee LP, Szema R. *Science*. 2005; 310:1148–1150. [PubMed: 16293752]
- [2]. Zorlutuna P, Annabi N, Camci-Unal G, Nikkhah M, Cha JM, Nichol JW, Manbachi A, Bae H, Chen S, Khademhosseini A. *Adv. Mater.* 2012; 24:1782–1804. [PubMed: 22410857]
- [3]. Ahn J-H, Kim H-S, Lee KJ, Jeon S, Kang SJ, Sun Y, Nuzzo RG, Rogers JA. *Science*. 2006; 314:1754–1757. [PubMed: 17170298]
- [4]. Brambley D, Martin B, Prewett PD. *Adv. Mater. Opt. Electron.* 1994; 4:55–74.
- [5]. Xia Y, Whitesides GM. *Annu. Rev. Mater. Sci.* 1998; 28:153–184.
- [6]. LaFratta CN, Li L, Fourkas JT. *Proc. NatL Acad. Sci. USA*. 2006; 103:8589–8594. [PubMed: 16720698]
- [7]. Jeon S, Malyarchuk V, Rogers JA, Wiederrecht GP. *Opt. Express*. 2006; 14:2300–2308. [PubMed: 19503567]
- [8]. Waits CM, Modafe A, Ghodssi R. *J. Micromech. Microeng.* 2003; 13:170–177.
- [9]. Jang J-H, Ullal CK, Maldovan M, Gorishnyy T, Kooi S, Koh C, Thomas EL. *Adv. Funct. Mater.* 2007; 17:3027–3041.
- [10]. Melchels FP, Feijen J, Grijpma DW. *Biomaterials*. 2009; 30:3801–3809. [PubMed: 19406467]
- [11]. Pfister A, Landers R, Laib A, Hubner U, Schmelzeisen R, Mulhaupt R. *J. Polym. Sci. Pol. Chem.* 2004; 42:624–638.
- [12]. Bensaoula A, Boney C, Pillai R, Shafeev GA, Simakin AV, Starikov D. *Appl. Phys. A*. 2004; 79:973–975.

- [13]. Park JY, Hwang CM, Lee SH. *Biomed Microdevices*. 2009; 11:129–133. [PubMed: 18670885]
- [14]. Chao SH, Carlson R, Meldrum DR. *Lab Chip*. 2007; 7:641–643. [PubMed: 17476386]
- [15]. Jackman RJ, Duffy DC, Ostuni E, Willmore ND, Whitesides GM. *Anal. Chem*. 1998; 70:2280–2287. [PubMed: 21644640]
- [16]. Stevens R, Miyashita T. *Imaging Sci. J*. 2010; 58:202–212.
- [17]. Choi YY, Chung BG, Lee DH, Khademhosseini A, Kim J-H, Lee S-H. *Biomaterials*. 2010; 31:4296–4303. [PubMed: 20206991]
- [18]. Girifalco LA, Good RJ. *J. Phys. Chem*. 1957; 61:904–909.
- [19]. Walther F, Davydovskaya P, Zurcher S, Kaiser M, Herburg H, Gigler AM, Stark RW. *J. Micromech. Microeng*. 2007; 17:524–531.
- [20]. Bhushan B. *Philos. Trans. R. Soc. A*. 2009; 367:1445–1486.
- [21]. Verpoorte E, De Rooij NF. *Proc. IEEE*. 2003; 91:930–953.
- [22]. Wu MC. *Proc. IEEE*. 1997; 85:1833–1856.
- [23]. Lee S-J, Kang H-W, Park JK, Rhie J-W, Hahn SK, Cho D-W. *Biomed Microdevices*. 2008; 10:233–241. [PubMed: 17885804]
- [24]. van der Meer AC, van der Berg A. *Integr. Biol*. 2012; 4:461–470.
- [25]. Berthier E, Young EWK, Beebe D. *Lab Chip*. 2012; 12:1224–1237. [PubMed: 22318426]
- [26]. Regehr KJ, Domenech M, Koepsel JT, Carver KC, Ellison-Zelski SJ, Murphy WL, Schuler LA, Alarid ET, Beebe DJ. *Lab Chip*. 2009; 2132–2139. [PubMed: 19606288]
- [27]. Huh D, Torisawa Y, Hamilton GA, Kim HJ, Ingber DE. *Lab Chip*. 2012; 2156–2164. [PubMed: 22555377]
- [28]. Huh D, Matthews BD, Mammoto A, Zavala MM, Hsin HY, Ingber DE. *Science*. 2010; 25:1662–1668. [PubMed: 20576885]
- [29]. Kim HJ, Huh D, Hamilton G, Ingber DE. *Lab Chip*. 2012; 12:2165–2174. [PubMed: 22434367]
- [30]. Carraro A, Hus W-M, Kulig KM, Cheung WS, Miller ML, Weinberg EJ, Swart EF, Kaazempur-Mofrad M, Borenstein JT, Vacanti JP, Neville C. *Biomed Microdevices*. 2008; 10:795–805. [PubMed: 18604585]
- [31]. Jang K-J, Suh K-Y. *Lab Chip*. 2010; 36–42. [PubMed: 20024048]
- [32]. Flemming RG, Murphy CJ, Arams GA, Goodman SL, Nealey PF. *Biomaterials*. 1999; 20:573–588. [PubMed: 10213360]
- [33]. Lee J, Cuddihy MJ, Kotov NA. *TISSUE ENG PT B-REV*. 2008; 14:61–86.
- [34]. Nikkhah M, Edalat F, Manouchen S, Khademhosseini A. *Biomaterials*. 2012; 21:5230–5246. [PubMed: 22521491]

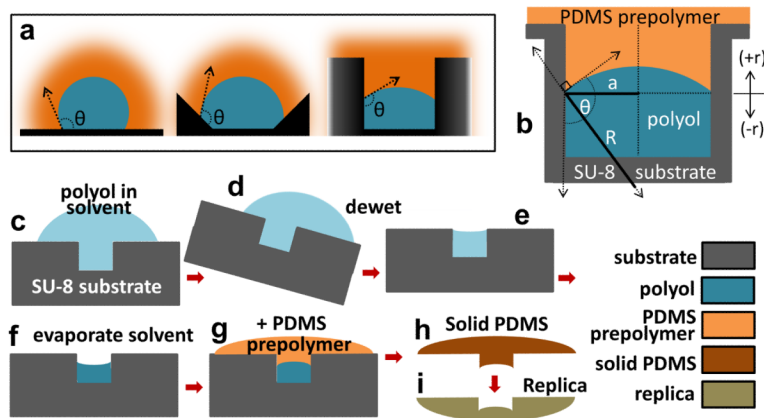
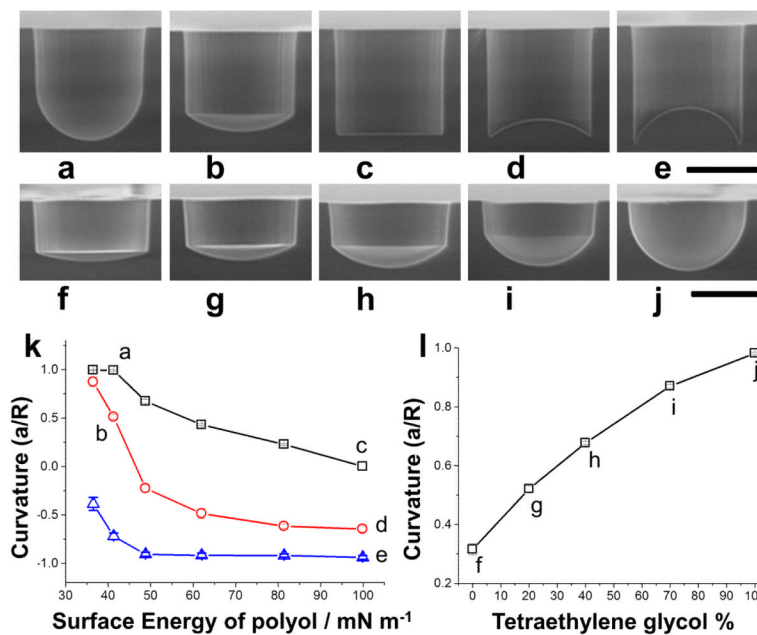


Figure 1. (a) Structured substrates direct placement of liquid volumes and immiscible liquid interfaces. (b) Definition of liquid/liquid/solid contact angle. When (b) represents a cylindrical microwell cross-section, $\cos(\theta)$ is numerically equivalent to the quantity a/R (microwell radius over meniscus radius). (c–i) An example of the liquid lithography process.

**Figure 2.**

Control of micropillar/microwell meniscus curvature via surface energy manipulation. (a–j) Cross-sections through PDMS microwells produced from replica molding off L.L.-made micropillars. (a–e) Microwells generated using different combinations of polyols and substrate surface treatments (a,b, tetraethylene glycol; c,d,e sorbitol; a,c SU-8; b,d and e, ethyl- and octyltrichlorosilane treated SU-8, resp.). (f–j), Microwells created with native SU-8 and a mixture of tetraethylene glycol and glycerol, at 0 (f), 20 (g), 40 (h), 70 (i), and 100 % (j) w/w TG/glycerol. (k) Coarse control of curvature using different combinations of polyols and substrate surface treatments. (l) Fine control of curvature using a mixture of tetraethylene glycol and glycerol. Error bars span two standard deviations on 9 measurements (k) and 4 measurements (l). Scale bars = 50 μm .

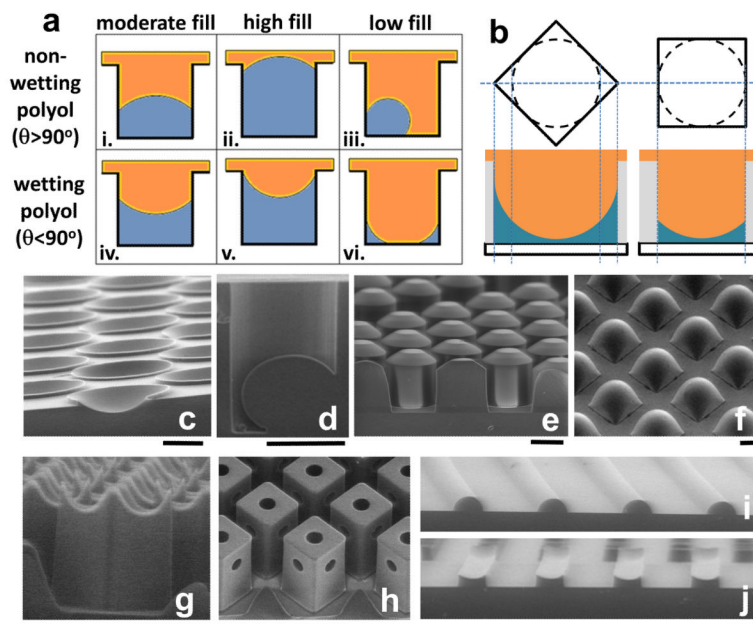


Figure 3. Increased structural complexity via manipulation of polyol fill volume and use of substrates with non-radially-symmetric features. (a) Schematic of the shape dependence on polyol filling level under wetting/non-wetting conditions. (b) Schematic showing the wicking behavior of a wetting polyol in high SA/V regions. (c–j) PDMS microstructures produced from substrates with simple recessed features under different wetting conditions and first liquid fill volumes. Scale bar = 50 μm .

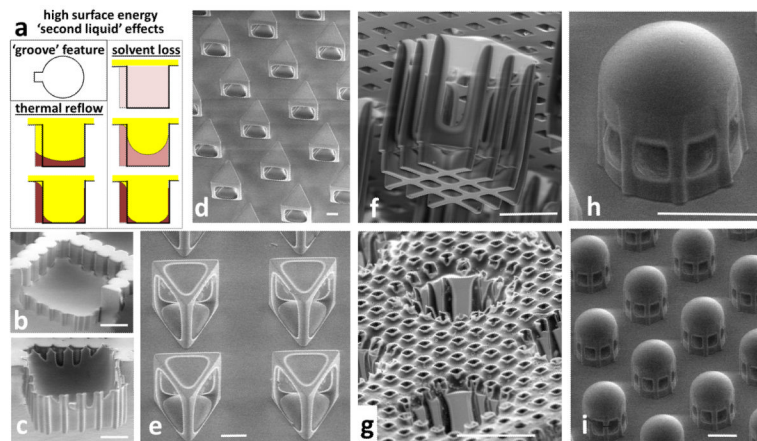


Figure 4.

(a) Schematic of liquid pushed into high SA/V features by overlaying high-surface energy liquid during thermal-initiated reflow (for SU-8) or concurrent with solvent loss (for PDLLA). (b,c) SU-8 in a notched PDMS microwell without (b) and with (c) thermal reflow. (d,e) SU-8 trigonal prism “cages” and “tables.” (f,g) PDLLA micro-patterned porous mesh. (h,i) SU-8 rotundas fabricated using two sequential L.L. operations. Scale bar = 50 μm in (b–f) and 100 μm in (g–i).